

Dual FRET molecular beacons for mRNA detection in living cells

Philip J. Santangelo, Brent Nix, Andrew Tsourkas and Gang Bao*

Department of Biomedical Engineering, Georgia Institute of Technology and Emory University, Atlanta, GA 30332, USA

Received December 24, 2003; Revised and Accepted March 24, 2004

ABSTRACT

The ability to visualize in real-time the expression level and localization of specific endogenous RNAs in living cells can offer tremendous opportunities for biological and disease studies. Here we demonstrate such a capability using a pair of molecular beacons, one with a donor and the other with an acceptor fluorophore that hybridize to adjacent regions on the same mRNA target, resulting in fluorescence resonance energy transfer (FRET). Detection of the FRET signal significantly reduced false positives, leading to sensitive imaging of K-ras and survivin mRNAs in live HDF and MIA PaCa-2 cells. FRET detection gave a ratio of 2.25 of K-ras mRNA expression in stimulated and unstimulated HDF, comparable to the ratio of 1.95 using RT-PCR, and in contrast to the single-beacon result of 1.2. We further revealed intriguing details of K-ras and survivin mRNA localization in living cells. The dual FRET molecular beacons approach provides a novel technique for sensitive RNA detection and quantification in living cells.

INTRODUCTION

The ability to detect, localize, quantify and monitor the expression of specific genes in living cells in real-time will offer unprecedented opportunities for advancement in molecular biology, disease pathophysiology, drug discovery and medical diagnostics (1). However, current methods for quantifying gene expression employ either selective amplification (as in PCR) or saturation binding followed by removal of the excess probes [as in microarrays and *in situ* hybridization (2)] to achieve specificity; neither approach is applicable when detecting gene transcripts within living cells. This requires the development of more sophisticated probes to distinguish signal from background with high sensitivity, convert target recognition directly into a measurable signal, and differentiate between true and false positive signals.

One possibility is to use molecular beacons, which are dual-labeled oligonucleotide probes with a reporter fluorophore at one end and a quencher at the other (3). These oligonucleotide probes are designed to form a stem-loop hairpin structure in

the absence of target, quenching the fluorophore reporter (4). Hybridization with a complementary target causes the hairpin to open, separating the fluorophore and quencher, and restoring fluorescence. This effectively converts target recognition into a fluorescence signal (5,6) with low background even in the presence of unbound probes. The hairpin structure also acts as an adjustable energy penalty for beacon opening which improves probe specificity (7,8).

When used within living cells, conventional molecular beacons can be degraded by nucleases or opened by nucleic acid binding proteins, leading to false positive signals (9–12). We report here the development of a novel detection approach which uses two molecular beacons whose fluorophores form a fluorescence resonance energy transfer (FRET) pair (13–16). The molecular beacons are designed to have sequences complementary to adjacent regions on the same mRNA target such that FRET only occurs when both beacons are hybridized to the target (Fig. 1). Using a reversible permeabilization method for fast and efficient cellular delivery, we demonstrate that this approach can lead to sensitive mRNA detection and localization in living cells, as illustrated with wild-type K-ras mRNA in normally growing and stimulated human dermal fibroblasts (HDF), and survivin mRNA in MIA PaCa-2 and HDF cells.

MATERIALS AND METHODS

Molecular beacon design and synthesis

To facilitate subsequent studies of early cancer detection, the K-ras-targeting molecular beacons were designed such that the donor beacon is complementary to a region of the K-ras gene containing codon 12 whose mutations are involved in many cancers. The survivin-targeting molecular beacons were designed such that the target sequence is unique, having no overlap with other genes in the IAP family. As shown in Table 1, a BHQ-2 quencher was attached to the 3'-end and a Cyanine 3 (Cy3) fluorophore was attached to the 5'-end of the random beacon and donor molecular beacons; a BHQ-3 quencher was attached to the 5'-end and a Cyanine 5 (Cy5) fluorophore was attached to the 3'-end of the acceptor molecular beacons. The probe lengths of K-ras-targeting donor and acceptor molecular beacons are, respectively 17 and 19 bases; the probe lengths of survivin-targeting donor and acceptor molecular beacons are 15 and 16 bases, respectively. The 'random' beacons have a probe length of 16 bases. All

*To whom correspondence should be addressed. Tel: +1 404 385 0373; Fax: +1 404 894 4243; Email: gang.bao@bme.gatech.edu

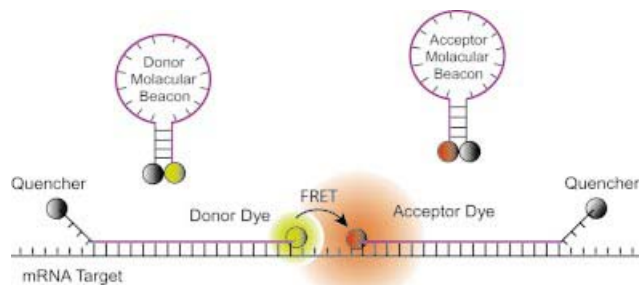


Figure 1. A schematic illustration showing the concept of dual FRET molecular beacons. Hybridization of donor and acceptor molecular beacons to adjacent regions on the same mRNA target results in FRET between donor and acceptor fluorophores upon donor excitation. By detecting FRET signal, fluorescence signals due to probe/target binding can be readily distinguished from that due to molecular beacon degradation and non-specific interactions.

molecular beacons are with the shared-stem design, with a stem length of five bases; they have an unmodified oligonucleotide backbone. The K-ras and survivin molecular beacons and Cy5 random beacon were synthesized by Biosource International (Camarillo, CA) and MWG Biotech (High Point, NC). The Cy3 random beacon and all of the synthetic targets were synthesized by Integrated DNA Technologies, Inc. (Coralville, IA).

Solution assays of probe-target hybridization

All solution studies of probe-target hybridization were carried out in a 1× PBS buffer without calcium and magnesium using a Safire fluorescent microplate fluorometer (Tecan, Zurich, Switzerland), with 545 nm Cy3 (donor) excitation and 560–680 nm emission detection. Concentrations of 200 nM donor, 200 nM acceptor molecular beacons and 200 nM target were used in a total volume of 50 µl.

Cell culture and stimulation

Normal HDF (Cambrex, NJ) were grown in Clonetics fibroblast growth medium supplemented with 2% fetal bovine serum (Cambrex, NJ), insulin, fibroblast growth factor, gentamicin sulfate and amphotericin-B. HDF cells used for stimulation studies were allowed to grow for 24 h before being starved with Clonetics fibroblast growth medium supplemented with 0.1% fetal bovine serum and no other supplements for 24 h. They were then stimulated with typical growth medium containing 20% fetal bovine serum. MIAPaCa-2 (ATCC, VA) pancreatic carcinoma cells were grown in DMEM supplemented with 10% FBS, 2.5% horse serum and 50 U/ml of penicillin and 50 µg/ml of streptomycin.

Molecular beacon delivery using reversible permeabilization

Molecular beacons were delivered into living cells using a reversible permeabilization method with streptolysin O (SLO), which was shown to be rapid, efficient, less damaging and more versatile (in terms of cell type) compared with conventional transfection methods (17). Specifically, SLO was activated first by adding 5 mM of TCEP to 2 U/ml of SLO for 30 min at 37°C. Cells grown in 24-well plates were incubated for 10 min in 200 µl of serum free medium

Table 1. Target sequences and the design of molecular beacons

Wild-type K-ras target (Bases 1–78)
5'-ATGACTGAATATAAACTTGTGGTAGTT
GGAGCTGGTGGCGTAGG
caag AGTGCCTTGACGATACAGC TAATTCAGAAT-3'
K-ras dual FRET molecular beacons
Donor MB: 5'-/Cy3/CCTACGACCAGCTCCGTAGG/BHQ-2/-3'
Acceptor MB: 5'-/BHQ-3/AGTGCGCTGTATCGTCAAGGCACT/Cy5/-3'
Survivin target (Bases 1–78)
5'-ATGGGTGCCCCGACGTTGCCCCCTGCC TGGCAGCCCTTTCTC
aagg ACCACCGCATCTCTAC ATTCAAGAACTGGCCC-3'
Survivin dual FRET molecular beacons
Donor MB: 5'-/Cy3/GAGAAAGGGCTGCCATTCTC/BHQ-2/-3'
Acceptor MB: 5'-/BHQ-3/ACCACGTAGAGATGCGGGT/Cy5/-3'
'Random' sequence target
5'-ATCGGTGCGCTGTGCG-3'
'Random' sequence molecular beacons
Donor MB: 5'-/Cy3/CACGTGACAAAGCGCACCGATACGTG/BHQ-2/-3'
Acceptor MB: 5'-/BHQ-3/ACGTGCGACAAAGCGCACCGATACGT/Cy5/-3'

Molecular Beacon (MB): underlined bases, bases added to create the stem domain. Target: lowercase bold, bases between two target sequences of the donor and acceptor beacon.

containing 0.2 U/ml of activated SLO (0.5 U SLO per 10⁶ cells) and 5 µl of each molecular beacon type for cell permeabilization and beacon delivery. Cells were then resealed by adding 0.5 ml of the typical growth medium and incubated for 1 h at 37°C before performing fluorescence microscopy imaging.

Fluorescence microscopy imaging

Fluorescence imaging of live cells was performed using a Zeiss Axiovert 100 TV epifluorescence microscope coupled to a Cooke Sensicam SVGA cooled CCD camera. For assays using dual FRET molecular beacons, excitation and emission detection were performed using 545 and 665 nm filters, respectively. For single beacon assays using either donor beacon alone, or the random beacons, a filter of 570 nm was used for fluorescence detection. An exposure time of 2 s was used for all imaging assays. Maximum signal to background ratios were calculated based on the maximum signal intensity in cells within the field of view divided by the average background pixel value from a portion of the field of view not containing any cell.

RT-PCR assay

Total RNA was isolated from HDF cells using a Qiagen RNeasy Mini Kit. The yield was 15 µg/ml for stimulated HDFs and 37 µg/ml for non-stimulated HDFs. The cDNA synthesis was performed using Invitrogen's ThermoScript RT-PCR kit with 150 ng of RNA and priming with random hexamers. The forward primer used for K-ras was GATTCCTACAGGAAGCAAGT, and reverse primer was TAATGGTGAATATCTTC. For GAPDH, the forward primer used was CCACCCATGGCAAATTCCATGGCA and the reverse primer was TCTAGACGGCAGGTCAGGTCCACC. PCR conditions were as follows: 95°C for 5 min, followed by 95°C for 30 s, 52°C for 30 s, and 72°C for 1 min (repeated for each cycle) with tubes removed after 15, 20, 25, 30, 35 and 40 cycles. Samples were run through on a 1% agarose gel and stained with EtBr.

Fluorescence *in situ* hybridization

Normal human dermal fibroblast cells were cultured in eight-well chambered cover slides for 24 h in normal growth medium (FGM-2, Cambrex Co.) and then washed with 1× PBS (without Ca or Mg). The slide was fixed in 100% methanol at -20°C for 10 min. After removing the methanol, the slides were allowed to air dry and stored overnight at -80°C. *In situ* hybridization assays were then performed by first washing the slides for 5 min in 1× PBS and hybridizing them overnight at 37°C in 1× PBS (no Ca or Mg) containing 400 nM of fluorescently labeled linear probes targeting wild-type K-ras (5'-Cy5-CCTACGCCACCAGCTCC-3') or as a control (5'-Cy5-AAAAAAAAAAAAAAAAAAA-3'). After removing the hybridization solution with washing and adding 1× PBS, the cells were imaged using an Axiovert 100 epi-fluorescent microscope.

RESULTS AND DISCUSSION

Dual FRET molecular beacons

Three molecular beacon FRET pairs were designed, synthesized and tested in solution. Each FRET probe pair consisted of two molecular beacons, one labeled with a donor fluorophore (donor beacon) and a second labeled with an acceptor fluorophore (acceptor beacon). These molecular beacons were designed to hybridize to adjacent regions on an mRNA target so that the two fluorophores will lie within the FRET range (~6 nm) when probe/target binding occurs for both beacons. Excitation of the donor fluorophore then results in fluorescence emission at a wavelength characteristic of the acceptor fluorophore, which serves as a positive FRET signal readily differentiable from non-FRET false positive signals due to probe degradation and non-specific probe opening (16). As shown in Table 1, dual FRET molecular beacon pairs were designed in a shared-stem fashion (18), i.e. the sequence of the fluorophore-attached arm of the stem (Fig. 1) is complementary to the target so that it participates in both stem formation and target hybridization. This design was chosen to help fix the relative distance between the donor and acceptor fluorophores and improve energy transfer efficiency. For all FRET molecular beacon pairs, Cy3 (peak excitation at 545 nm) and Cy5 (peak emission at 665 nm) were used as the donor and acceptor fluorophores, respectively, and BHQ-2 and BHQ-3 were used as quenchers for the donor and acceptor molecular beacons, respectively. One pair of molecular beacons targets a segment of the wild-type K-ras gene (Table 1) whose codon 12 mutations are involved in the pathogenesis of many cancers (19). A member of the GTPase family, K-ras is involved in regulating cell growth, proliferation and differentiation (20). As shown in Table 1, the target sequence for K-ras-targeting donor beacon has 17 bases, and that for the acceptor beacon has 19 bases. The other pair of molecular beacons targets the survivin gene, which is a member in the inhibitor of apoptosis protein (IAP) family (21). The target sequences for survivin-targeting donor and acceptor molecular beacons are, respectively, 15 bases and 16 bases long. For both K-ras- and survivin-targeting molecular beacon pairs, the stem size is five bases, and the gap size between the donor and acceptor beacons on a target is four bases. For use in negative controls, we also designed Cy3- and

Cy5-labeled 'random'-sequence molecular beacons ('random beacon') whose specific 16-base target sequence does not match with any mammalian gene. Note that both the donor (Cy3-labeled) and acceptor (Cy5-labeled) random beacons have an identical sequence, and the 'random sequence' target is for a signal beacon only (Table 1).

Solution studies of FRET signal and specificity

In-solution probe-target hybridization studies were carried out to determine the extent of energy transfer between, and signal-to-background ratio of, dual FRET molecular beacons, as well as the specificity of the random beacon. Shown in Figure 2A are five fluorescence emission spectra of molecular beacons targeting wild-type K-ras under Cy3 excitation (545 nm); they were generated by having: (i) donor beacons only in the presence of target (blue curve), representing the signal of a single beacon assay; (ii) both donor and acceptor beacons in solution with target (green curve), representing the FRET signal; (iii) donor beacons only without target (red curve), representing the background of a single-beacon assay; (iv) donor and acceptor beacons in solution without target (light blue curve), representing the background of a FRET assay and (v) acceptor beacons with target (black curve). These results imply that, even when a large amount of single (donor or acceptor) molecular beacons are degraded by nucleases or open due to non-specific interactions, the resulting fluorescence signal at the FRET detection wavelength of 665 nm (light blue curve) is still much lower than the FRET signal (green curve). The FRET signal-to-background ratio (green curve versus light blue curve at 665 nm) is approximately 9.0. The survivin-targeting molecular beacons under Cy3 excitation (545 nm) exhibited essentially the same spectroscopic features, as shown by the five curves in Figure 2B. When the 'random' beacons were mixed, respectively, with the complementary random-sequence target, or the wild-type K-ras target, or the survivin target, only targets complementary to the probe sequence of random beacons gave a strong fluorescence signal, other targets gave very low background (Fig. 2C), confirming the high specificity of random sequence molecular beacons.

K-ras mRNA detection in normally-growing and stimulated HDF cells

In order to demonstrate the advantages of the dual FRET molecular beacon approach, living cell assays were performed with both normally growing and stimulated HDF cells. To increase the K-ras mRNA expression level, HDF cells were first starved for 24 h and then stimulated with serum for 8 h before molecular beacon delivery (22). Cells were permeabilized using streptolysin O (SLO) (17) and were exposed to either Cy3-labeled random-sequence or K-ras-targeting single molecular beacons, or Cy3- and Cy5-labeled random-sequence or K-ras-targeting donor and acceptor molecular beacon pairs. The resulting fluorescence signal was observed under Cy3 excitation (545 nm) 1 h after beacon delivery with the Cy3 emission channel (570 nm) for single beacon assays and Cy5 emission channel (665 nm) for dual beacon assays (Fig. 3). Signals from the single random beacon negative controls (Fig. 3A and C) should be due entirely to beacon degradation, non-specific interactions and possibly other backgrounds such as autofluorescence of the cell. Signals

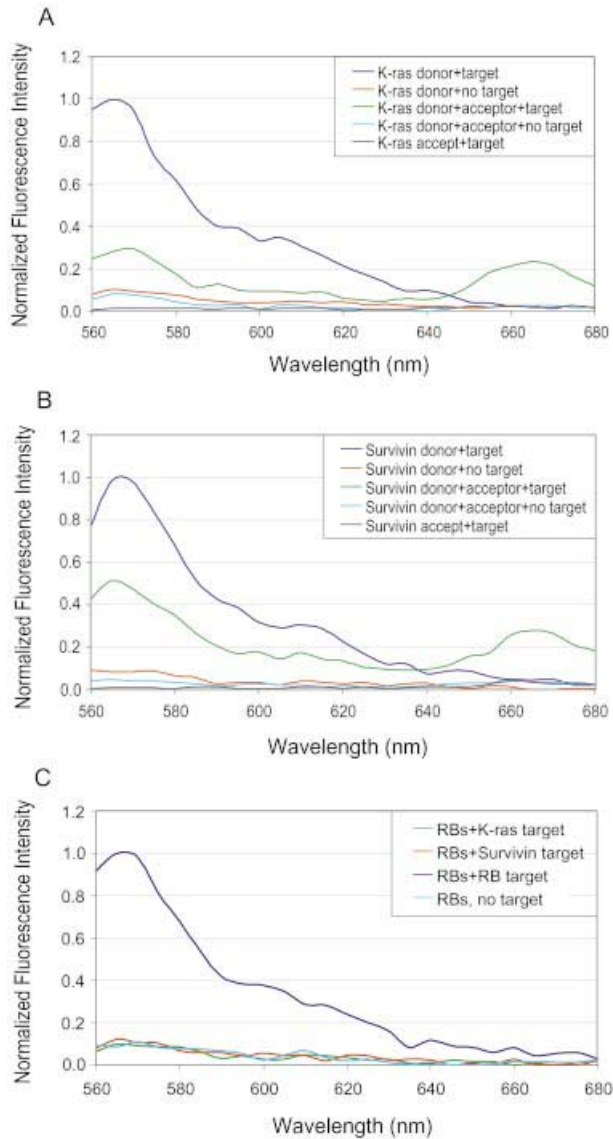


Figure 2. Solution studies of probe-target hybridization of dual FRET molecular beacons. (A) Fluorescence emission spectra of K-ras targeting molecular beacons under Cy3 excitation (545 nm). The blue curve was generated by having donor beacons only in the presence of target, representing the signal of a single beacon assay. The red curve was a result of having donor beacons only without target, representing the background of a single-beacon assay. The green curve was due to both donor and acceptor beacons in solution with target, representing the FRET signal. The light blue curve was due to both donor and acceptor beacons in solution without target, representing the background of a FRET assay. The black curve was a result of having acceptor beacons only in the presence of target, representing the background signal of single acceptor beacons. A high signal-to-background ratio was obtained at the peak FRET signal (~665 nm). (B) Emission spectra for survivin-targeting molecular beacons, with the four curves defined as in (A). (C) Emission spectra for 'random sequence' molecular beacons (RBs) with, respectively, complementary targets (blue curve), survivin targets (red curve), K-ras targets (green curve) and no target (light blue curve), indicating very high hybridization specificity.

from single Cy3-labeled (i.e. unpaired donor) K-ras-targeting molecular beacons (Fig. 3B) were not appreciably greater than those found with random beacons (Fig. 3A), clearly demonstrating the limitation of using single molecular

beacons in RNA detection in living cells, especially when the expression level is relatively low. With stimulated HDF cells, the fluorescence signal level in single beacon K-ras detection increased (Fig. 3D), but it was still not much higher than the corresponding background signal (Fig. 3C).

When random beacon FRET pairs were delivered into either normally growing or stimulated HDF cells, the resulting FRET signals detected in the Cy5 channel were very low (Fig. 3E and G). The expression levels of K-ras mRNA in normally growing and stimulated HDF cells were detected using the dual FRET molecular beacons, and the resulting fluorescence signals are shown in Figure 3F and H, respectively. Even with unstimulated HDF cells, the fluorescence signal as a result of K-ras mRNA detection (Fig. 3F) was much higher than the background (Fig. 3E), indicating that dual FRET molecular beacons are capable of distinguishing true and false positive signals, which is in sharp contrast with the results of single beacon detection shown in Figure 3A and B. With stimulated HDF cells, the fluorescence signal level as a result of the dual FRET molecular beacon detection of K-ras mRNA had a significant increase, as shown in Figure 3H. Quantitative analysis of the average signal intensities of the images in Figure 3F and H gave a factor of 2.25 increase in K-ras expression in stimulated HDF compared with that in normally growing cells, consistent with the result of the RT-PCR assay, which indicated a factor of 1.95 increase in K-ras expression after stimulation. In contrast, single-beacon detection assays yielded an increase of only a factor of 1.2 (Fig. 3I). This clearly demonstrates that the dual FRET molecular beacons approach has much better detection sensitivity and allows for a more quantitative measurement of relative changes in mRNA level in living cells upon stimulation. This capability is important for both basic biological studies and drug discovery research in which it is critical to quantify changes of gene expression in living cells in response to stimuli including hormones, growth factors, candidate drug molecules and other chemical/mechanical insults.

In comparing the ratios of K-ras mRNA expression in stimulated and unstimulated HDF cells, we made the assumption that the K-ras expression level in different cells imaged simultaneously is roughly the same, which is supported by Figure 3B, D, F and H. Consequently, although the quantitative analysis of fluorescence intensity was performed based on, and averaged over, only a few cells, the results should remain valid when a large number of cells are examined. Therefore, we believe that the ratios of 1.2 (single-beacon) and 2.25 (dual-beacon) given in Figure 3I represent fairly accurately the difference in K-ras mRNA detection using single and dual molecular beacon approaches. Further, we believe that the result of dual-beacon FRET detection is more accurate than that of the single-beacon approach, since it yielded a much lower background signal as demonstrated by Figure 3A, C, E and G. However, when specific mRNA expression has large variations from cell to cell, analyses of fluorescence intensity of only a few cells may not be statistically significant and the results may not be reproducible. In this case, the fluorescence intensity of a large number of cells (say, at least a few hundred cells) must be analyzed in order to obtain accurate quantification of mRNA expression.

Survivin mRNA expression in normal and cancerous cells

To detect survivin mRNA expression in HDF and MIAPaCa-2 cells, survivin-targeting donor beacon alone, survivin-targeting dual FRET molecular beacons, and the random beacons (Table 1) were delivered, respectively, into these cells using SLO. The resulting fluorescence signal was visualized 1 h after delivery. Figure 4A and C displays the fluorescence

signal of random beacons in HDF and MIAPaCa-2 cells, respectively, representing the background signal level in each cell type with single beacon detection. When the fluorescence of single (unpaired) survivin-targeting donor beacons were imaged under Cy3 excitation (545 nm) and Cy3 emission detection (570 nm), the signal level in MIAPaCa-2 cells (Fig. 4B) was similar to that of random beacon (Fig. 4A), indicating that the signal was mainly due to false positive events. The fluorescence signal of single survivin-targeting molecular beacons in HDF cells was essentially the same as that of the random beacon. Therefore, using single beacons, the true signal of survivin mRNA detection cannot be distinguished from false positive signals.

Using FRET detection, i.e. with Cy3 excitation and Cy5 emission detection, the signal generated by random beacons was very low in both HDF and MIAPaCa-2 cells, as can be seen from Figure 4E and G. This implies that the false positive signals due to beacon degradation and non-specific opening can be dramatically reduced using FRET optics. We found that, using dual FRET molecular beacons targeting survivin (Table 1), and with the FRET optics (i.e. 545 nm excitation and 570 nm emission detection), the fluorescence signal level in MIAPaCa-2 cells (Fig. 4F) was much higher than that in HDF cells (Fig. 4H), with a 250% increase in average signal intensity. This demonstrates that dual FRET molecular beacons have the ability to quantify specific mRNA expression in different cell populations.

Localization of K-ras and survivin mRNA in living cells

We found that the dual FRET molecular beacons approach can give a clear and detailed picture of mRNA localization in living cells which may reveal important information on mRNA processing, transport and protein production. To demonstrate, in Figure 5A and B, fluorescence images of K-ras mRNA in stimulated HDF cells are shown, indicating an intriguing localization pattern. Evidently, the K-ras mRNA molecules were not randomly distributed but rather well organized and localized in the cytoplasm. It is clear from the fluorescence images that the K-ras mRNA molecules were well distributed in the cytoplasm and followed the cell morphology as indicated by the cable-like portion of an elongated cell in Figure 5B. When the fluorescence image of a

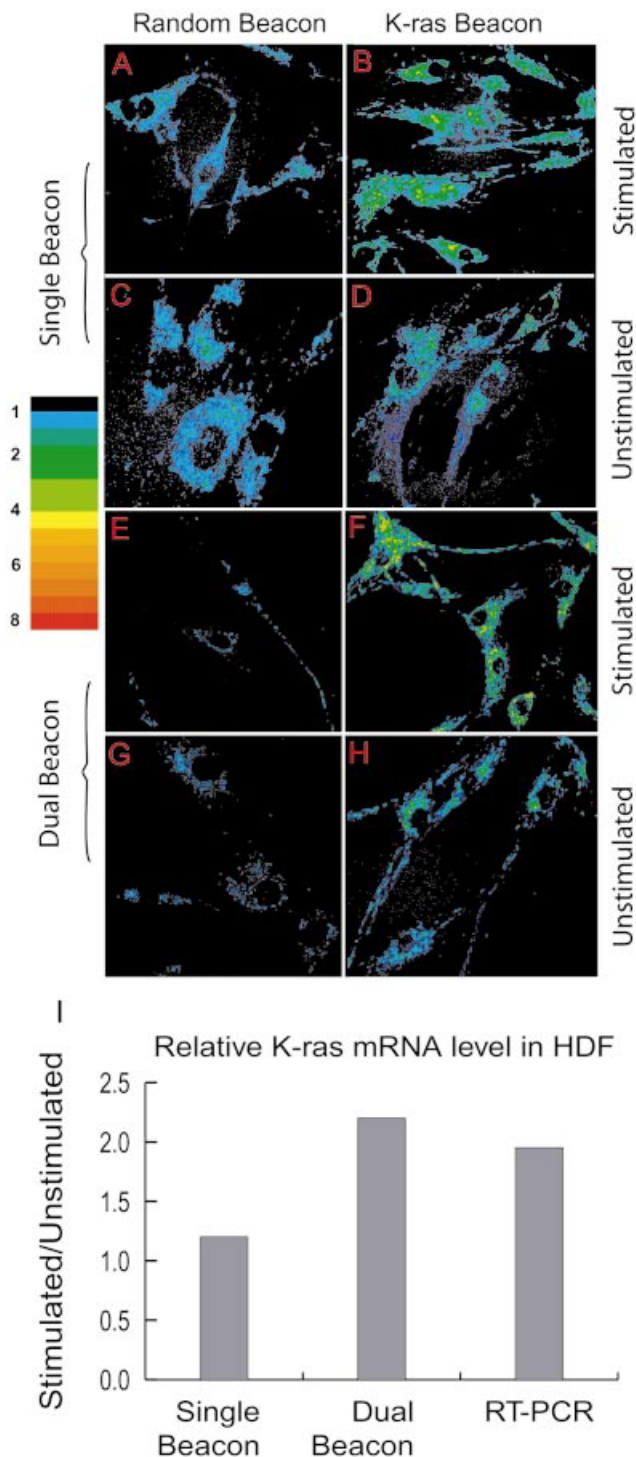


Figure 3. Detection of K-ras mRNA expression in normally-growing and stimulated HDF cells using single donor molecular beacons only (A–D), or dual FRET molecular beacons (E–H). (A and C) Fluorescence signal of single ‘random’ sequence molecular beacons in (A) normally-growing and (C) stimulated HDF cells, respectively, representing the background due to beacon degradation and non-specific interactions. (B and D) Fluorescence signal due to single K-ras targeting donor beacons in (B) normally growing and (D) stimulated HDF cells under Cy3 excitation (545 nm) and emission detection (570 nm). Note that when single beacons were used with unstimulated cells the K-ras signal level in (B) was similar to that of the background in (A). (E and G) Fluorescence signal of two ‘random’ sequence molecular beacons in (E) normally growing and (G) stimulated HDF cells, respectively, under Cy3 excitation (545 nm) and FRET detection (665 nm), representing the background in dual FRET beacon assays. (F and H) Fluorescence signal due to K-ras targeting dual FRET molecular beacons in (F) normally growing and (H) stimulated HDF cells using FRET optics (i.e. 545 nm excitation and 665 nm emission detection). The dual FRET molecular beacons gave a much better signal-to-background ratio, and a more quantitative measure of mRNA expression level (I).

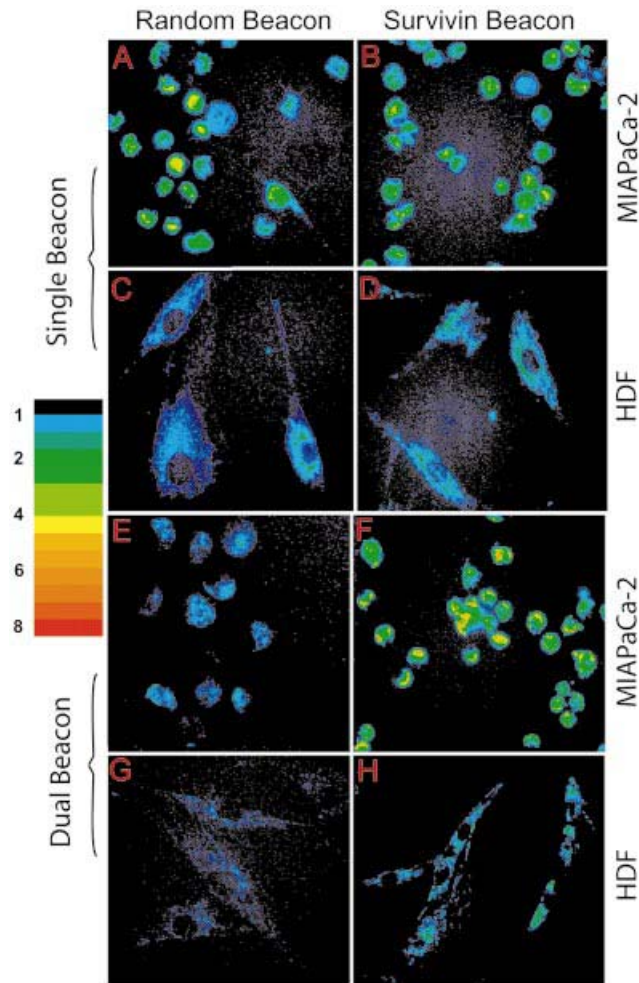


Figure 4. Detection of survivin mRNA expression in MIAPaCa-2 and normal HDF cells using single donor molecular beacons only (A–D), or dual FRET molecular beacons (E–H). (A and C) Fluorescence signal of single ‘random’ sequence molecular beacons in (A) MIAPaCa-2 and (C) normal HDF cells, respectively, representing the background due to beacon degradation and non-specific interactions. (B and D) Fluorescence signal in Cy3 channel due to single survivin-targeting donor beacons in (B) MIAPaCa-2 and (D) HDF cells. Note that single survivin-targeting molecular beacons gave a signal level similar to the background. (E and G) Fluorescence signal of two ‘random’ sequence molecular beacons in (E) MIAPaCa-2 and (G) HDF cells, respectively, using FRET optics, representing the background signal in FRET-based assays. (F and H) Fluorescence signal due to survivin-targeting dual FRET molecular beacons in (F) MIAPaCa-2 and (H) HDF cells using FRET optics. The dual FRET molecular beacons gave a much better signal-to-background ratio, and could give better quantification in survivin mRNA expression level in MIAPaCa-2 and HDF cells.

small peripheral region of a cell is expanded, the K-ras mRNAs seem to be localized along a cytoskeletal filament system, possibly the microtubule system. Indeed the co-localization of mRNA with cytoskeletal filaments has been suggested (23,24). A similar feature is shown in Figure 5B in which the image of a small region of a different HDF cell is expanded. We believe that this is the first direct visualization of K-ras mRNA localization in living cells. Surprisingly, we found that survivin mRNA localized in MIAPaCa-2 cell very differently. As shown in Figure 5C in which the fluorescence image was superimposed with a white light image of the cells,

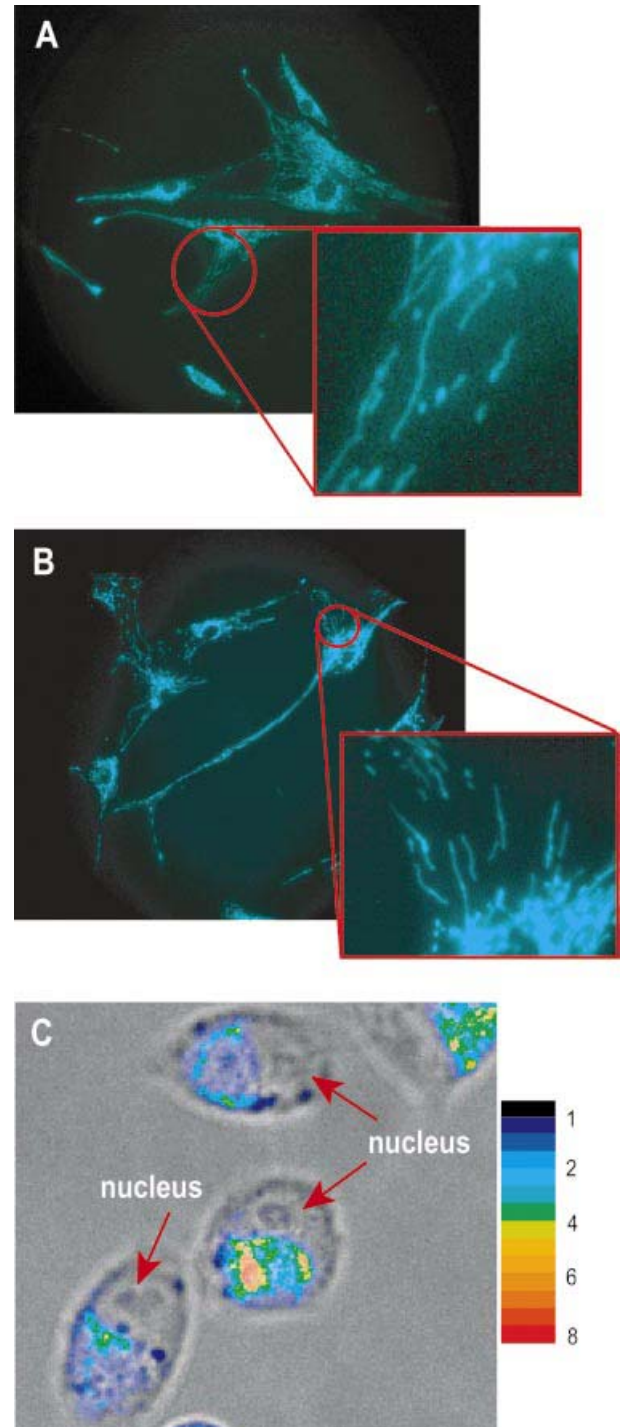


Figure 5. mRNA localization in HDF and MIAPaCa-2 cells. (A and B) Fluorescence images of K-ras mRNA in stimulated HDF cells. Note the filamentous K-ras mRNA localization pattern. (C) A fluorescence image of survivin mRNA localization in MIAPaCa-2 cells. Note that survivin mRNAs localized to one side of the nucleus of the MIAPaCa-2 cells.

survivin mRNAs seemed to localize in a non-symmetrical pattern within MIAPaCa-2 cells, often to one side of the nucleus of the cell. The intriguing differences in mRNA localization is likely a consequence of the association of mRNA with the cell cytoskeleton (24) or mitochondria (25).

Control study using *in situ* hybridization

As a control, we performed a fluorescence *in situ* hybridization (FISH) assay detecting K-ras mRNA in fixed HDF cells. We used a fluorescently labeled linear probe (5'-Cy5-CCTACGCCACCAGCTCC-3') that has the same probe sequence as the K-ras-targeting donor molecular beacon (Table 1). As demonstrated in Figure 6A, the fluorescence image obtained in the FISH assay of K-ras mRNA detection in HDF cells gave a filamentous localization pattern as well, especially in the cell peripheral region, similar to that shown in Figure 5A and B, confirming that the mRNA localization revealed in this study is true. However, in the region near the cell nucleus, the fluorescence image as a result of FISH has a high background compared with that of living cell assays using dual FRET molecular beacons. Since the probes entered both the cell cytoplasm and nucleus during FISH, a strong and diffused fluorescence signal appeared in the fixed HDF cell nuclei (Fig. 6A). As a negative control, we performed a FISH assay with fluorescently labeled linear Poly-A probes (5'-Cy5-AAAAAAAAAAAAAAAAAAAA-3') and the resulting background signal was very low, as can be seen from Figure 6B. This further confirmed that the fluorescence signal observed in our live cell and fixed cell studies of specific mRNA detection was truly due to probe/target hybridization.

Intracellular distribution of probe/target binding sites

It should be noted that in all of the images shown in Figures 3–5, very little mRNA expression was detected in the cell nucleus. Although our results seemingly contradict the observation that antisense oligonucleotide probes rapidly accumulate in the nucleus (26–28), it remains to be seen if such nuclear localization is due to any fundamental biological reason. In fact, when molecular beacons were microinjected into cells, considerably more fluorescence signal was observed in the cytoplasm than nucleus (6). It is also possible that the intracellular distribution of signal is related to the specific delivery method used. For example, when delivered via the endocytic pathway (e.g. liposome-based transfection), antisense oligonucleotide probes tend to be trapped inside endocytic vesicles and degraded in the endosomes and lysosomes (29,30). In this study, we used a toxin-based delivery method so that the probes do not go through endosomes or lysosomes after entering cells through membrane permeabilization. We believe that after internalization, the probes bind to their mRNA targets in the cytoplasm before reaching the nucleus. The probe concentrations we used are significantly lower (at least a factor of 10 lower) than in most of the antisense work (31); therefore, the probability of driving the probes into the nucleus by a high concentration gradient is much smaller. As a control, we have delivered fluorescently labeled linear oligonucleotides using SLO and most of the signal observed was in the cytoplasm as well (data not shown).

It has been revealed over the last few years that RNA molecules have a much wider range of functions, from physically conveying and interpreting the genetic information of living cells, to essential catalytic roles, to providing structural support for molecular machines, to gene silencing. These activities are controlled by the dynamics of both the expression levels of specific RNAs and their spatial distributions. Although *in vitro* assays such as DNA microarrays and

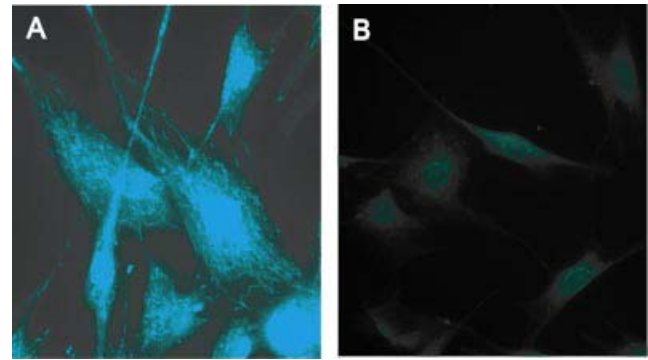


Figure 6. Fluorescence *in situ* hybridization (FISH) studies. (A) Detection of K-ras mRNA in fixed HDF cells using fluorescently labeled linear probes. Note the filamentous localization pattern near the cell peripheral region. (B) A negative control study of the FISH assay using fluorescently labeled linear Poly-A probes resulted in very low background.

northern blotting can reflect the relative changes in RNA expression level of a cell population, imaging of specific RNA (including mRNA and microRNA) in living cells in real time can provide essential information on how external stimuli alter the gene expression level in cells, what are the processes of RNA localization, transport and interference, and how RNAs interact with proteins or protein complexes. As demonstrated here, the dual FRET molecular beacons technique can detect endogenous mRNA in living cells rapidly with high specificity, sensitivity and signal-to-background ratio, thus providing a powerful tool to address all these issues. For example, in drug discovery, this method can be used in high-throughput assays to quantify and monitor the dose-dependent changes of specific mRNA expression in response to different candidate drug molecules. In basic biological studies, this method will allow researchers to visualize the dynamics and localization of specific RNAs.

A very intriguing observation in this study is the localization of mRNA in living cells. As demonstrated in Figure 5, K-ras mRNAs displayed an interesting filament-like localization pattern in HDF cells, with a clear indication of spreading out in the cytoplasm and following the cell morphology. On the other hand, survivin mRNA was localized on one side of the cell nucleus. But why are K-ras and survivin mRNAs localized in such a peculiar way? What are the biological implications of such localization? RNA localization is an evolutionarily conserved phenomenon and may be the first step in targeting proteins to specific locations to facilitate protein–protein interactions (32). For example, mRNA localization and translation has been found in dendrites and axons in neural cells (33). It has been indicated that intracellular mRNA localization may involve interactions between targeting signals within the RNA, motor molecules and the cytoskeleton (34). Although the association of mRNA with microtubules has been suggested based on the results of biochemical assays, there is still a lack of direct confirmation of mRNA localization to cytoskeletal filaments. One difficulty is that the cytoskeleton is a dynamic network and the mechanism of transport for mRNA is largely unknown. Studies have been performed using either GFP fusion proteins that bind to RNA (35) or by injecting fluorescently labeled mRNAs into cells

and tracking them (36). However, by imaging endogenous mRNAs directly we will be able to gain insights into the rates of RNA synthesis and processing, the dynamics of RNA transport and localization, and RNA–protein interactions.

As demonstrated in this study, the dual FRET molecular beacons approach has the advantage that false positive signals in living cell gene detection due to nucleases and nucleic acid binding proteins can be significantly reduced or even eliminated, leading to high detection sensitivity. This approach is based on simultaneous hybridization of two probes to the same mRNA target so that a FRET signal can be emitted upon proper excitation. Although dual FRET linear probes have been used for living cell mRNA detection (37), they typically provide a higher background signal than molecular beacons as a result of the fluorescence emission of unbound probes, including donor emission at the detection wavelength and direct acceptor excitation. Further, hairpin probes can provide better specificity, as analyzed in Tsourkas *et al.* (38). While the use of dual FRET probes may further increase detection specificity, compared with single molecular beacon assays, the dual-probe approach does require twice as many probes to be delivered into cells and a longer time for probe targeting and hybridization. Therefore, for specific applications where fast detection (~30 min) is crucial, single molecular beacon assays such as that based on peptide-linked molecular beacons (30) may be more suitable.

As demonstrated in previous studies, the use of 2'-*O*-methyl modified molecular beacons has certain potential advantages including improved intracellular stability and faster probe/target hybridization kinetics (39). However, there are issues and potential drawbacks as well. One issue is that the 2'-*O*-methyl modified molecular beacons may be more prone to open in living cells due to nucleic acid binding proteins (12), therefore generating a higher background. Further, 2'-*O*-methyl modified beacons are RNA-like, and therefore may form double-stranded RNA upon probe–target binding and trigger unwanted RNAi in living cells. A major advantage of using 2'-*O*-methyl molecular beacons is their enhanced nuclease resistance. However, most of the nucleases are in the endosomes, lysosomes and nucleus (40). If the probes are delivered directly into the cytoplasm and the endocytic pathway can be avoided, nuclease resistance may not be an essential issue. Although we chose to use unmodified molecular beacons in this study, it is important to compare the performance of molecular beacons with different backbone modifications in living cell gene detection (P.J.Santangelo and G.Bao, unpublished work).

A critical issue in living cell mRNA detection is target accessibility, which is largely controlled by mRNA secondary and tertiary structures and RNA-binding proteins. Specifically, mRNA in a cell almost always has proteins bound to it, which may alter mRNA structure and prevent probe hybridization. Therefore, in selecting the probe sequences of the dual FRET molecular beacons, it is important to avoid targeting sequences that are 'buried' inside the tertiary structure or where double-stranded RNA is formed. Although predictions of mRNA secondary structure can be made using existing software (e.g. *mfold*), they may not be accurate due to limitations of the biophysical models used. Further, we only have very limited knowledge of the sequences occupied dynamically by RNA-binding proteins.

Therefore, for each gene to target, it is often necessary to select multiple unique sequences along the target RNA, and have corresponding molecular beacons designed, synthesized and tested in cells to achieve high signal-to-background ratio.

Another important issue in living cell gene detection is the quantification of mRNA expression in single cells. There are many challenges in obtaining an accurate measure of the number of mRNA molecules per cell using molecular beacons (or any imaging method). For example, it is necessary to distinguish true and background signals, determine the fraction of mRNA molecules hybridized with probes, and quantify the possible self-quenching effect of the reporter, especially when mRNA is highly localized. Since the fluorescence intensity of the reporter may be altered by the intracellular environment, it is also necessary to create an internal control by, for example, injecting fluorescently labeled oligonucleotides with known quantity into the same cells and obtaining the corresponding fluorescence intensity (37).

A related issue in molecular beacon based gene quantification in living cells is the detection sensitivity, which is dictated not only by probe/target hybridization but also by the properties of fluorophore, fluorescence detection method, optical imaging instrumentation (microscope and camera) and background signal. As a result of the low background in the dual FRET molecular beacons approach, improved detection sensitivity can be achieved compared with FISH, as demonstrated by Figures 4 and 6. Using microinjection of probe/target duplexes, Sokol *et al.* found that the molecular beacon based approach could detect 10 mRNA molecules per cell (6) when they are concentrated at the same spot. It is estimated that the current approach can reliably detect a few hundred copies of endogenous mRNA per cell in single cell gene detection. With the use of advanced fluorophores such as quantum dots (41) or lanthanide chelates (16), fluorescence detection methods such as time-resolved FRET, and more sensitive optical imaging instruments such as that with photon counting, it is possible to detect as low as 1–5 copies of mRNA molecules in a single cell. An alternative approach is to obtain the average mRNA expression over a large number of cells (say one million), similar to that in RT–PCR studies. In this case, a FRET-based flow cytometry assay using Fluorescence Activated Cell Sorter (FACS) could be performed to detect the fluorescence signal level in living cells. While single cell mRNA detection can be used to study more accurately the variation of gene expression in a cell population with different stages in the cell cycle or different disease states, the determination of the average mRNA expression level over a large number of cells may be advantageous in that, when the cell–cell variation of mRNA expression is large, it is statistically more significant and thus more reproducible compared with the mRNA level detected using a relatively small number of cells.

ACKNOWLEDGEMENTS

The authors acknowledge helpful discussions with Mark Behlke and Nitin Nitin. This work was supported in part by NSF (BES-0222211), and by DARPA-AFOSR (F49620-03-1-0320).

REFERENCES

1. Tsien, R.Y. (2003) Imaging imaging's future. *Nat. Rev. Mol. Cell Biol.*, **4**, ss16–21.
2. Femino, A.M., Fay, F.S., Fogarty, K. and Singer, R.H. (1998) Visualization of single RNA transcripts *in situ*. *Science*, **280**, 585–590.
3. Tyagi, S. and Kramer, F.R. (1996) Molecular beacons: probes that fluoresce upon hybridization. *Nat. Biotechnol.*, **14**, 303–308.
4. Bernacchi, S. and Mely, Y. (2001) Exciton interaction in molecular beacons: a sensitive sensor for short range modifications of the nucleic acid structure. *Nucleic Acids Res.*, **29**, e62.
5. Tyagi, S., Bratu, S.P. and Kramer, F.R. (1998) Multicolor molecular beacons for allele discrimination. *Nat. Biotechnol.*, **16**, 49–53.
6. Sokol, D.L., Zhang, X., Lu, P. and Gewirtz, A.M. (1998) Real time detection of DNA:RNA hybridization in living cells. *Proc. Natl Acad. Sci. USA*, **95**, 11538–11543.
7. Bonnet, G., Tyagi, S., Libchaber, A. and Kramer, F.R. (1999) Thermodynamic basis of the enhanced specificity of structured DNA probes. *Proc. Natl Acad. Sci. USA*, **96**, 6171–6176.
8. Tsourkas, A., Behlke, M.A., Rose, S.D. and Bao, G. (2003) Hybridization kinetics and thermodynamics of molecular beacons. *Nucleic Acids Res.*, **31**, 1319–1330.
9. Mitchell, P. (2001) Turning the spotlight on cellular imaging. *Nat. Biotechnol.*, **19**, 1013–1017.
10. Li, J.J., Geyer, R. and Tan, W. (2000) Using molecular beacons as a sensitive fluorescence assay for enzymatic cleavage of single-stranded DNA. *Nucleic Acids Res.*, **28**, e52.
11. Dirks, R.W., Molenaar, C. and Tanke, H.J. (2001) Methods for visualizing RNA processing and transport pathways in living cells. *Histochem. Cell Biol.*, **115**, 3–11.
12. Molenaar, C. *et al.* (2001) Linear 2' O-Methyl RNA probes for the visualization of RNA in living cells. *Nucleic Acids Res.*, **29**, e89.
13. Cardullo, R.A., Agrawal, S., Flores, C., Zamecnik, P.C. and Wolf, D.E. (1988) Detection of nucleic acid hybridization by nonradiative fluorescence resonance energy transfer. *Proc. Natl Acad. Sci. USA*, **85**, 8790–8794.
14. Sixou, S., Szoka, F.C., Jr, Green, G.A., Giusti, B., Zon, G. and Chin, D.J. (1994) Intracellular oligonucleotide hybridization detected by fluorescence resonance energy transfer (FRET). *Nucleic Acids Res.*, **22**, 662–668.
15. Bratu, D.P., Cha, B.J., Mhlanga, M.M., Kramer, F.R. and Tyagi, S. (2003) Visualizing the distribution and transport of mRNAs in living cells. *Proc. Natl Acad. Sci. USA*, **100**, 13308–13313.
16. Tsourkas, A., Behlke, M.A., Xu, Y. and Bao, G. (2003) Spectroscopic features of dual fluorescence/luminescence resonance energy transfer molecular beacons. *Anal. Chem.*, **75**, 3697–3703.
17. Faria, M. *et al.* (2001) Phosphoramidate oligonucleotides as potent antisense molecules in cells and *in vivo*. *Nat. Biotechnol.*, **19**, 40–44.
18. Tsourkas, A., Behlke, M.A. and Bao, G. (2002) Structure–function relationships of shared-stem and conventional molecular beacons. *Nucleic Acids Res.*, **30**, 4208–4215.
19. Minamoto, T., Mai, M. and Ronai, Z. (2000) K-ras mutation: Early detection in molecular diagnosis and risk assessment of colorectal, pancreas and lung cancers — A review. *Cancer Detect. Prev.*, **24**, 1–12.
20. Hancock, J.F. (2003) Ras proteins: different signals from different locations. *Nat. Rev. Mol. Cell Biol.*, **4**, 373–384.
21. Altieri, D.C. (2003) Survivin and apoptosis control. *Adv. Cancer Res.*, **88**, 31–52.
22. Quinoces, A.F. and Leon, J. (1995) Serum growth factors up-regulate H-ras, K-ras and N-ras proto-oncogenes in fibroblasts. *Cell Growth Differ.*, **6**, 271–279.
23. Bassell, G. and Singer, R.H. (1997) mRNA and cytoskeletal filaments. *Curr. Opin. Cell Biol.*, **9**, 109–115.
24. Hesketh, J.E. (1996) Sorting of messenger RNAs in the cytoplasm: mRNA localization and the cytoskeleton. *Exp. Cell Res.*, **225**, 219–236.
25. Johnson, P.R., Dolman, N.J., Pope, M., Vaillant, C., Petersen, O.H., Tepikin, A.V. and Erdemli, G. (2003) Non-uniform distribution of mitochondria in pancreatic acinar cells. *Cell Tissue Res.*, **313**, 37–45.
26. Leonetti, J.P., Mechti, N., Degols, G., Gagnor, C. and Lebleu, B. (1991) Intracellular distribution of microinjected antisense oligonucleotides. *Proc. Natl Acad. Sci. USA*, **88**, 2702–2706.
27. Lorenz, P., Misteli, T., Baker, B.F., Bennett, C.F. and Spector, D.L. (2000) Nucleocytoplasmic shuttling: a novel *in vivo* property of antisense phosphorothioate oligodeoxynucleotides. *Nucleic Acids Res.*, **28**, 582–592.
28. Dias, N. and Stein, C.A. (2002) Antisense oligonucleotides: basic concepts and mechanisms. *Mol. Cancer Ther.*, **1**, 347–355.
29. Dokka, S. and Rojanasakul, Y. (2000) Novel non-endocytic delivery of antisense oligonucleotides. *Adv. Drug Deliv. Rev.*, **44**, 35–49.
30. Nitin, N., Santangelo, P.S., Kim, G., Nie, S. and Bao, G. (2004) Peptide-linked molecular beacons for efficient delivery and rapid mRNA detection in living cells. *Nucleic Acids Res.*, **32**, e58.
31. Lloyd, B.H., Giles, R.V., Spiller, D.G., Grzybowski, J., Tidd, D.M. and Sibson, D.R. (2001) Determination of optimal sites of antisense oligonucleotide cleavage within TNF α mRNA. *Nucleic Acids Res.*, **29**, 3664–3673.
32. Kloc, M. and Billinski, S.M. (2003) RNA localization and its role in the spatially restricted protein synthesis. *Folia Histochem. Cytobiol.*, **41**, 3–11.
33. Job, C. and Eberwine, J. (2001) Localization and translation of mRNA in dendrites and axons. *Nat. Rev. Neurosci.*, **2**, 889–898.
34. Tekotte, H. and Davis, I. (2002) Intracellular mRNA localization: motors move messages. *Trends Genet.*, **18**, 636–642.
35. Singer, R.H. (2003) RNA localization: visualization in real-time. *Curr. Biol.*, **13**, R673–675.
36. Chudakov, D.M. *et al.* (2003) Kindling fluorescent proteins for precise *in vivo* photolabeling. *Nat. Biotechnol.*, **21**, 191–194.
37. Tsuji, A., Koshimoto, H., Sato, Y., Hirano, M., Sei-Iida, Y., Kondo, S. and Ishibashi, K. (2000) Direct observation of specific messenger RNA in a single living cell under a fluorescence microscope. *Biophys. J.*, **78**, 3260–3274.
38. Tsourkas, A., Behlke, M.A., Rose, S.D. and Bao, G. (2003) Hybridization kinetics and thermodynamics of molecular beacons. *Nucleic Acids Res.*, **31**, 1319–1330.
39. Tsourkas, A., Behlke, M.A. and Bao, G. (2003) Hybridization of 2'-O-methyl and 2'-deoxy molecular beacons to RNA and DNA targets. *Nucleic Acids Res.*, **30**, 5168–5174.
40. Price, N.C. and Stevens, L. (1999) *Fundamentals of Enzymology*, 3rd edn. Oxford University Press, Oxford, UK.
41. Chan, W.C. and Nie, S. (1998) Quantum dot bioconjugates for ultrasensitive nonisotopic detection. *Science*, **281**, 2016–2018.